Fracture mechanics model for predicting fatigue strength of metallic alloys containing large second phase particles

Zerbst, U.[1,a] Madia, M.[2,b] and Hellmann, D.[3,c]

[1] Federal Institute for Materials Research and Testing (BAM), 9.1, D-12205 Berlin, Germany

[2] Politecnico di Milano, Department of Mechanical Engineering, I-20165 Milano, Italy

[3] Helmhotz-Zentrum, Institute of Materials Research, D-21502 Geesthacht

[a] uwe.zerbst@bam.de [b] mauro.mdia@polimi.it [c] dieter.hellmann@hzg.de

Keywords: fatigue strength, S-N curve, fracture mechanics, crack propagation, short cracks

Abstract: An analytical fracture mechanics model for predicting finite life fatigue strength of components is presented which combines a number of well established and newly developed approaches such as Murakami's and McEvily's approach for describing the transient behaviour of crack closure of short cracks, the analytical (long) crack closure function of Newman, the R6 procedure modified by a method for improving the ligament yielding correction proposed by the authors and other elements. Basic assumption is the pre-existence of initial flaws such that the crack initiation or nucleation stage is small and can be neglected. The application of the model is demonstrated for small tension plates of aluminium Al 5380 H321 with artificial initial defects generated by FIB technology, the size of which was fixed on the basis of fractographic investigations on broken, smooth specimens.

1. Stages of Lifetime of Components Subjected to Cyclic Loading

The lifetime of a cyclically loaded component can be roughly subdivided into three stages: crack initiation, fatigue crack propagation and fracture. Frequently the crack initiation stage is defined such that it covers nucleation and early crack propagation until the crack reaches some tenth of a millimetre at surface. However, a closer look reveals that this phase can be subdivided in a number of sub-stages (e.g. [1]):

(a) The crack initiation sub-stage in a narrower sense which is characterised by the accumulation of microscopic plastic deformation sometimes occurs at the smooth surface but more frequently it happens at scratches, pores, inclusions and similar defects which act as micro-notches and/or due to strain concentration zones caused by different stiffness properties of defect and matrix material. In the case of very high cycle fatigue (fracture after 10^8 loading cycles or more) initiation takes place subsurface but also at material defects [2].

(b) Subsequent to crack initiation the crack size is in the range of micro-structural features such as the grain size. Its propagation is characterised by a irregular crack front and alternating phases of acceleration and retardation or even crack arrest. The arrest of the largest of a number of initially growing cracks is associated with the fatigue limit phenomenon [3].

(c) With the increasing crack size the effect of the micro-structure on local fatigue crack propagation diminishes and the propagation rate becomes rather steady. When the crack size reaches the order of mechanical discontinuities such as the plastic zone size or a notch stress field the crack is designated as mechanically short. Its propagation, in principle, can be described by classical fracture mechanics, however not by the linear elastic ΔK concept. As the micro-structurally short

crack also the mechanically short one can be arrested under constant applied loading due to the gradual build-up of the plasticity-induced crack closure phenomenon.

(d) Long cracks propagate above a crack-size independent long-crack threshold ΔK_{th}. Their growth can be described by the da/dN-ΔK curve concept when the crack closure phenomenon is taken into account. For crack propagation under constant amplitude loading this is state-of-the-art today. The long crack propagation is terminated by the fracture of the component.

The different stages and sub-stages of fatigue crack propagation are schematically illustrated in Fig. 1.

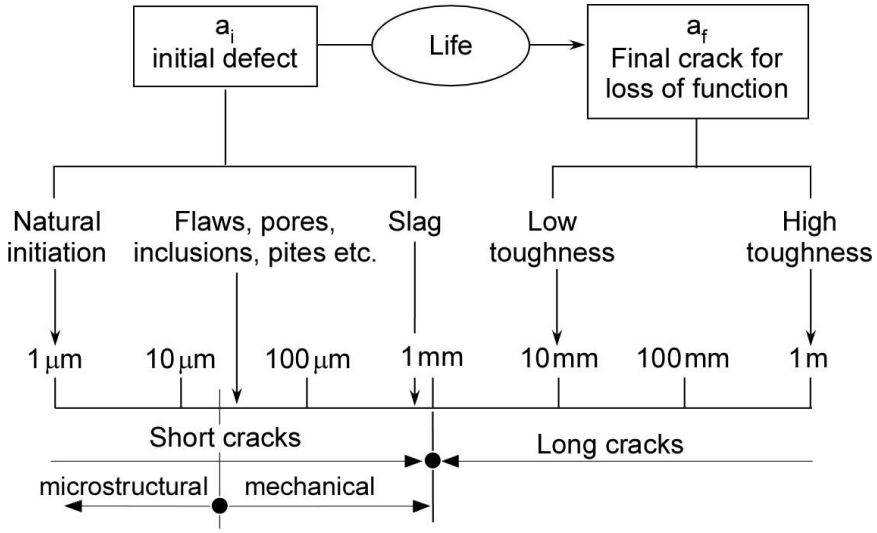

Fig. 1: Stages of fatigue crack propagation of cyclically loaded componets (acc. to [4]; slightly modified)

It is essential in the context of the present paper that the crack initiation sub-stage in the narrower sense frequently is very limited for many engineering materials. Instead of a detailed discussion a statement of Polak in Elsevier's"Comprehensive Structural Integrity" shall be cited here: "Numerous studies have shown that in the majority of materials and under normal loading conditions, the period of crack initiation in smooth specimens without defects amounts to less than 5-20% of the fatigue life. In materials containing defects, the fraction of life spent in crack initiation is even lower. The major part of the life is spent in the growth of cracks, namely in the growth of short cracks." [1]. This fact allows to model metallurgical initial defects as cracks without yielding over-conservative lifetime predictions.

2. Model Proposed for Predicting Finite-life Fatigue Strength and Lifetime

The observation that the essential part of fatigue lifetime of many engineering materials is covered by short crack growth requires a fracture mechanics model which is able to describe this stage in an adequate manner. The authors proposed such a model in [5] where the reader can also find a more detailed description as it is possible here due to limited space. The model, for a number of partial aspects, uses and combines otherwise established approaches because of which there exist similarities with alternative models (e.g. [6-9]) which also cannot be discussed here in any detail. Instead, the reader is referred to [5]. Fig. 2 summarises the input and model parameters and the analysis steps of the present procedure.

In the following the analysis steps shall be exemplarily explained for tension plates of aluminium alloy Al 5083 H 321 used for some first validation.

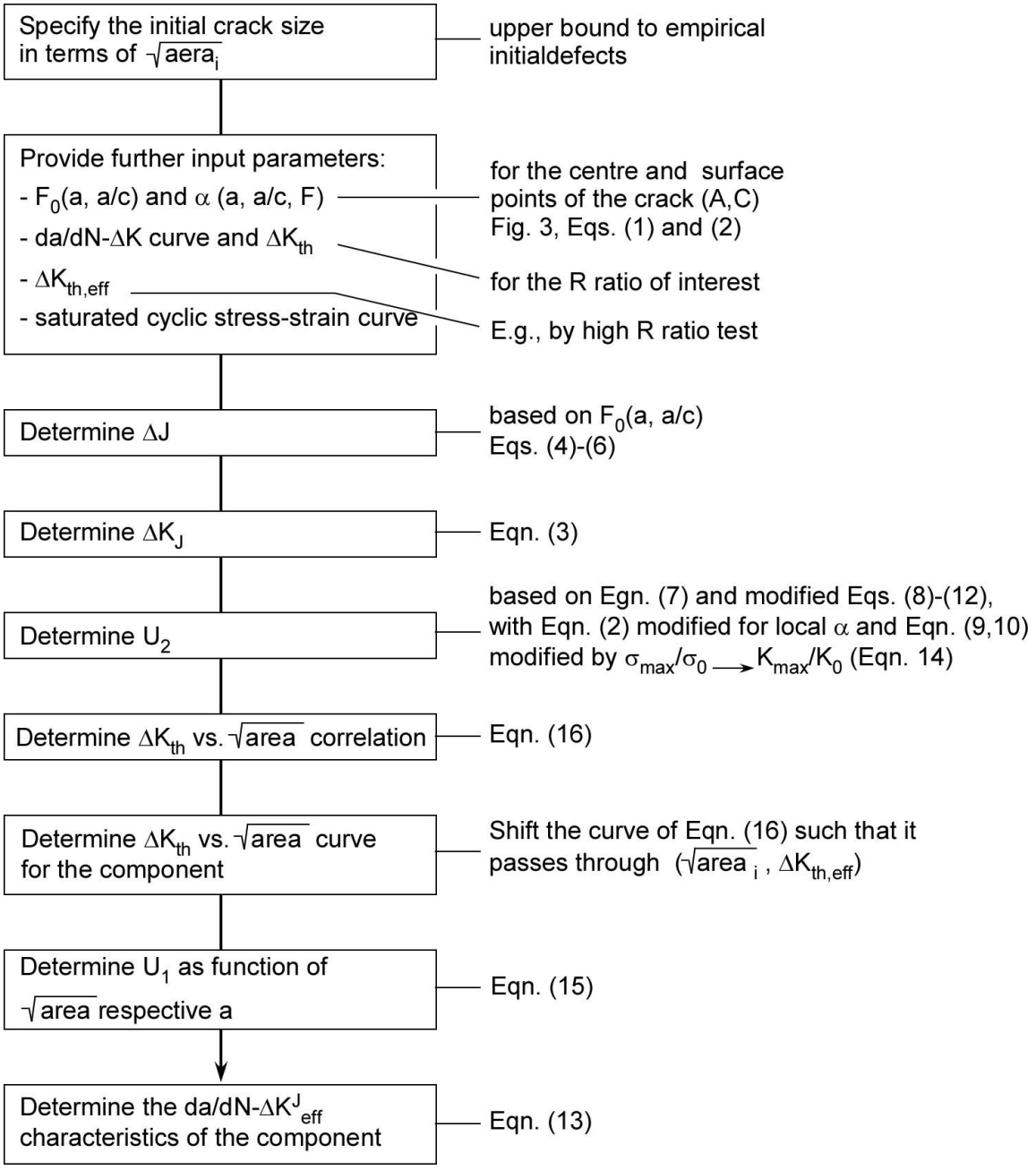

Fig. 2: Input and model parameters and steps of the fracture mechanics model presented here.

2.1 Initial crack size: Different to the so-called EIFS concept (EIFS = Equivalent Initial Flaw Size) (e.g. [10,11]) the initial crack size is not obtained by backward-calculation but is independently determined. For the present study fracture surfaces of the cyclically tension loaded plates were fractographically analysed. The dimensions of the plates are given in Fig. 3. A fracture surface containing an initial defect is shown along with a micrograph section and statistics of the defect sizes found on all specimens in Fig. 4.

In Fig. 4(d), following a proposal of Murakami (e.g. [2]), the initial crack size is given as the square root of its area, $\sqrt{area}$, with the index "i" standing for "initiation". Note that individual fractographic determination of $\left(\sqrt{area}\right)_i$ cannot be afforded in regular application. Therefore, some fixed values in the frame of a classification scheme have to be elaborated in the future, at least for application at the lowest of a number of analysis levels with stepwise decreasing conservatism.

The statistical upper bound of the defect depth was found to be in the order of 50 μm which is quite typical for aluminium alloys [11].

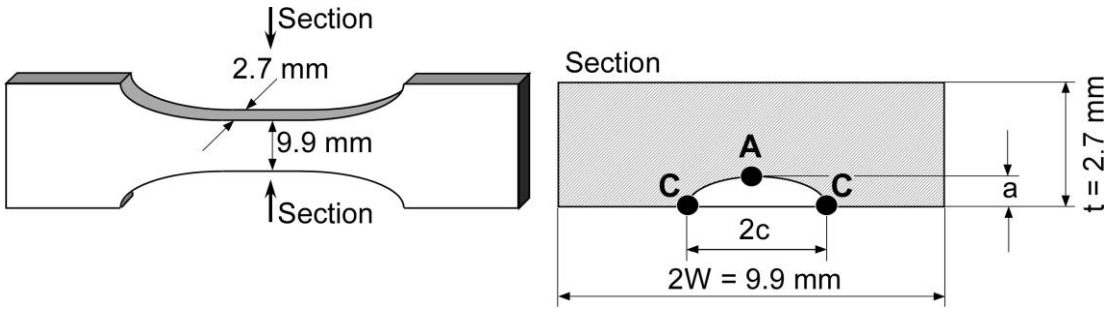

Fig. 3: Schematic plot of the tensile specimens used for determining the initial defect size distribution and for the generation of the S-N curve with artificial FIB (Focused Ion Beam) cracks.

2.2 Material properties: The material properties needed as input parameters of the proposed model comprise the da/dN-ΔK curve for the stress ratio $R = K_{min}/K_{max}$ of interest (in the present case R = 0.2), the long crack fatigue threshold ΔK_{th} for the same R, the intrinsic threshold (no plasticity-induced crack closure) and the stabilised cyclic stress-strain curve. The Paris range of the da/dN-ΔK curve, $da/dN = C \cdot \Delta K^n$, was experimentally determined for R = 0.2 on four specimens. The average value of C was $C = 4.05 \cdot 10^{-12}$ (ΔK in $MPa\sqrt{mm}$; da/dN in mm/loading cycle) for an n assumed as n = 3. The threshold values for R = 0,2 und R → 1 (intrinsic value) were 1.5 $MPa\sqrt{m}$ and 0.925 $MPa\sqrt{m}$ respectively (Fig. 5). The stabilised cyclic stress-strain curve is given in Fig. 6.

2.3 Model parameters: The model parameters of the analysis were the linear elastic stress intensity factor K for points A and C at the crack front (Fig. 3) which were obtained by the solution of Raju and Newman [12] and confirmed by finite elements; reference loads F_0 and local constraint factors α, both also for points A and C.
5

Following a proposal of the authors in [13] the reference load F_0 replaces the limit load in assessment procedures such as R6 [14] or SINTAP [15]. It is defined as that load at which the ligament plastification $L_r = F/F_0 = 1$. This may be different for different positions at the crack front. Approximating finite element results, an analytical F_0 solution for the configuration of Fig. 3 loaded in tension was obtained:

$$F_0 = \alpha \cdot W \cdot t \cdot \left[1 - \beta \frac{a \cdot c}{W}\right] \sigma_y \qquad (1)$$

with $\beta = \begin{cases} 0.276\ mm^{-1} & \text{Point A} \\ 0.271\ mm^{-1} & \text{Point C} \end{cases}$, $\alpha \approx 2$; $\alpha = 1.884 + \frac{\sigma_Y}{\sigma_0}$ and $\sigma_0 = 2900$ MPa

(for a = 35 μm – 2,2 mm; a/t = 0,013 – 0,81; $R_{p0,2}$ = 186 – 503 MPa).

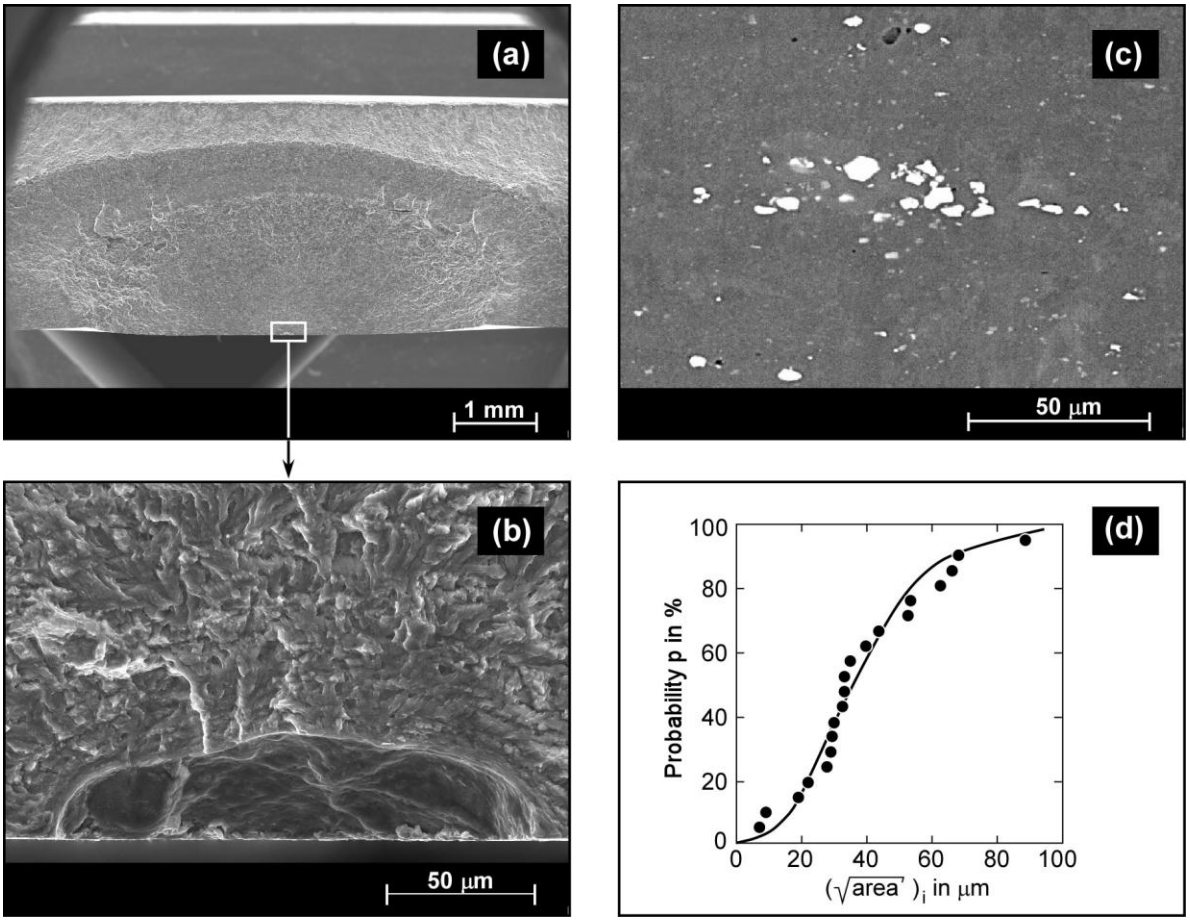

Fig. 4: Initial defects in the material AL5380 H321, fractographic and metallographic investigations: (a) and (b) example for an initial defect; (c) a cluster of inclusions with increased concentration of manganese, iron and nickel; (d) statistical distribution of the initial crack depth.

A local constraint parameter α was determined instead of the global value according to Newman [16] the latter being given by Eqn. (2):

$$\alpha_g = \frac{1}{A_T} \sum_{m=1}^{M} \left(\frac{\sigma_{yy}}{\sigma_0} \right)_m A_m \qquad (2)$$

(A_m = projected area of a yielded element m on the uncracked ligament, σ_{yy}/σ_0 = normalized crack opening stress for the element m, A_T = total projected area of all elements (M) which have yielded)

The parameter has been obtained by finite elements as a local parameter separately for points A and C of the semi-elliptical surface crack by modifying the Eqn. (2) such that the total area of the plastic zone ahead of the crack, A_T, is replaced by local areas around the two points of interest. A more detailed description of the concrete realisation is found in [17]. The resulting α values are given as tables in [5].

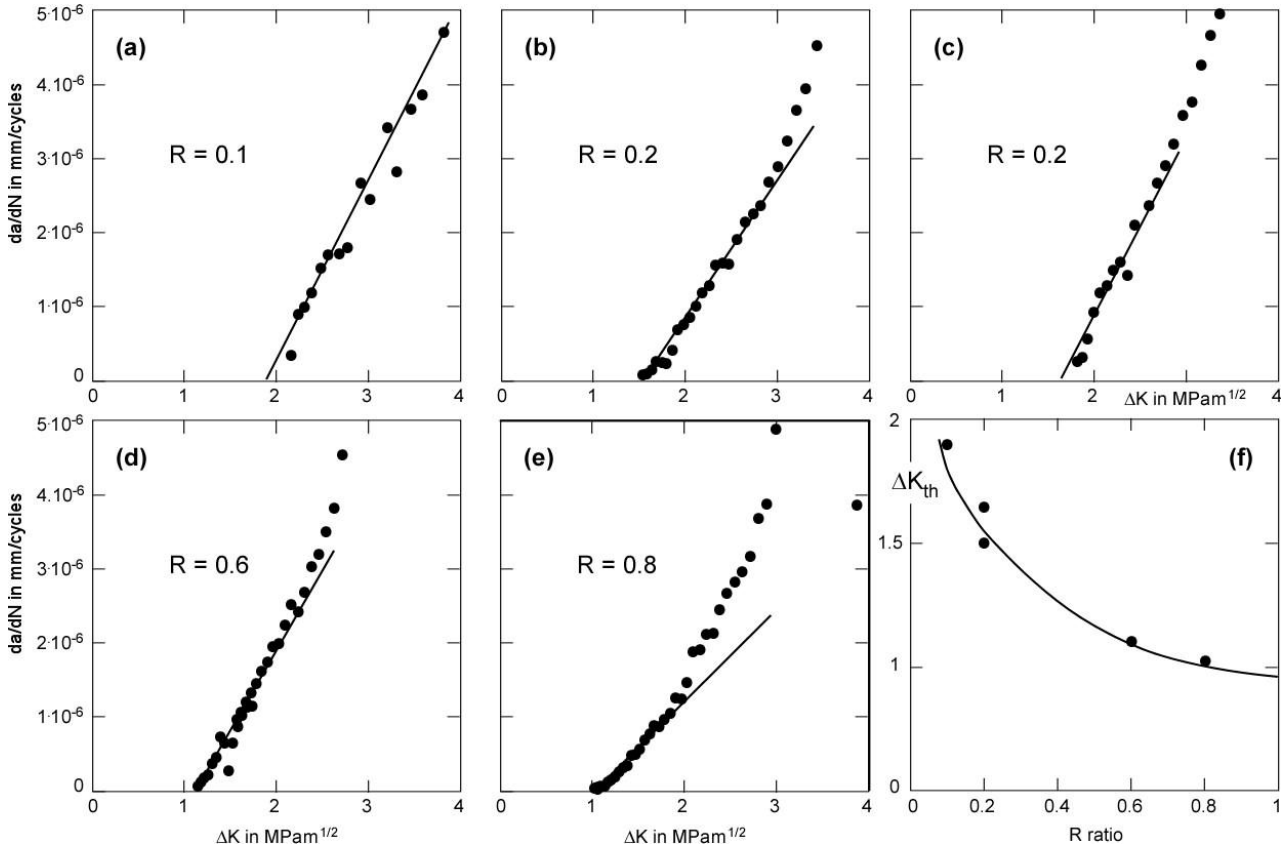

Fig. 5: Determination of the intrinsic threshold value $\Delta K_{th,eff}$ for the material AL5380 H321: (a) to (e) Determination of ΔK_{th} for R ratios of 0.1, 0.2, 0.6 and 0.8; (f) Determination of $\Delta K_{th,eff}$ by extrapolating the ΔK_{th} values of (a) – (e) to R = 1.

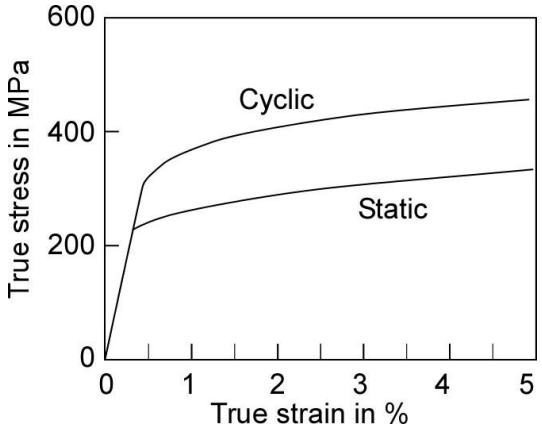

Fig. 6: Static and cyclic stress strain curve of the material AL5380 H321 used in the present validation study.

2.4 Crack driving force of mechanically short cracks: The considerations in this paper mainly focus on short crack propagation (see Section 1). This is no problem insofar as the maximum initial defect sizes found in at the fracture surfaces (see Fig. 4d) are sufficiently large not to be micro-structurally short cracks any more. It has already been mentioned that mechanically short cracks cannot adequately been described by the ΔK concept since the size of the plastic zone ahead of the crack is in the same order as the crack length. In order to address the local yielding effect ΔK is replaced by a ΔK^J which is formally obtained as

$$\Delta K^J = \sqrt{\Delta J \cdot E'}$$

$$E' = \begin{cases} E & \text{plane stress} \\ E/\left(1-\nu^2\right) & \text{plane strain} \end{cases} \tag{3}$$

With respect to a discussion of the cyclic J integral, ΔJ, the reader is referred to [5]. Within this paper a (slightly modified) approach of McClung [18,19] is applied by which ΔJ is determined by

$$\Delta J = \frac{\Delta K^2}{E'} \cdot \left[f\left(\Delta L_r\right)\right]^{-2} \tag{4}$$

$$\text{with } \Delta L_r = \frac{\Delta F}{2F_Y} = \frac{\Delta \sigma_{ref}}{2\sigma_Y}. \tag{5}$$

$$\text{and } L_r = F/F_0 . \tag{6}$$

2.5 Modelling the plasticity-induced crack closure pheneomenon:

With respect to modelling the crack closure effect it has to be distinguished between long cracks (the effect is completely build-up) and short cracks (the effect is still gradually developing). Crack closure is described by a parameter U (U_1 – short crack; U_2 – long crack). For the long crack the so-called NASGRO equation is used which is based on results obtained by applying the modified strip yield model of Newman [21]:

$$U_2 = \frac{\Delta K_{eff}}{\Delta K} = \frac{1-f}{1-R} \tag{7}$$

$$\text{with } f = \frac{\sigma_{open}}{\sigma_{max}} = \begin{cases} A_0 + A_1 R + A_2 R^2 + A_3 R^3 & \text{for } R \geq 0 \\ A_0 + A_1 R & \text{for } -2 < R < 0 \end{cases} \tag{8}$$

The coefficients A_i are given by

$$A_0 = \left(0.825 - 0.34\alpha_g + 0.05\alpha_g^2\right)\left[\cos\left(\frac{\pi/2 \cdot \sigma_{max}}{\sigma_0}\right)\right]^{\left(1/\alpha_g\right)} \tag{9}$$

$$A_1 = \left(0.415 - 0.071\alpha_g\right)\frac{\sigma_{max}}{\sigma_0} \tag{10}$$

$$A_2 = 1 - A_0 - A_1 - A_3 \tag{11}$$

$$A_3 = 2A_0 + A_1 - 1 \tag{12}$$

For the present model Eqs. (7) to (12) have been modified in several aspects:

(a) The ΔK parameter is replaced by ΔK^J. The determination of the parameter is as described above. The complete modified crack propagation equation is then:

$$\frac{da}{dN} = C\left(\Delta K_{eff}^J\right)^n = C\begin{cases} \left(U_1 \Delta K^J\right)^n & a_i < a < a^* \\ \left(U_2 \Delta K^J\right)^n & a_i \geq a^* \end{cases} \tag{13}$$

(b) Originally the f function in Eqn. (8) has been obtained for centre-cracked plates subjected to uniform tension. The question arises whether it can also be applied to other configurations, for example bending geometries. McClung at al. [22] (see also [19]) carried out extended finite element investigations on M(T) center-cracked plates in tension, SE(T) single-edge-cracked plates in

tension, SE(B) single-edge-cracked plates in bending and pure bending geometries and concluded that the f-function and, as a consequence, the crack opening stress σ_{open} (or K_{op}) are more accurately correlated by the K_{max}/K_0 ratio than by σ_{max}/σ_0 in Eqs. (9) and (10). They proposed to substitute the latter by K_{max}/K_0:

$$\frac{K_{max}}{K_0} = \frac{Y\sigma_{max}\sqrt{\pi a}}{\sigma_0\sqrt{\pi a}} \tag{14}$$

Other authors [14,23] have also found K_{max}/K_0 to be a superior parameter. Therefore, it is adopted in the present study too.

(c) The constraint parameter α in Eqs. (9) and (10) is not used as a fixed parameter as in the NASGRO approach but determined by finite element analyses based on Eqn. (2), but determined as local parameter for points A and C of the crack.

(d) The reference stress σ_0 in Eqs. (9), (10) and (14) is not chosen as the average of the quasi-static yield and tensile strength as in NASGRO but as the cyclic yield strength (Fig. 6).

With respect to the gradual build-up of the plasticity-induced crack closure effect for the short crack stage the model assumes that the latter is mirrored in the development of the short crack fatigue threshold (as e.g. in [7]). The parameter U_1 can then be determined by

$$U_1 = \frac{U_2}{\Delta K_{th}(a)/\Delta K_{th,lc}} \tag{15}$$

with the index „lc“ designating the long crack. The ΔK_{th}-crack depth function is described by an approach of McEvily et al. [25]

$$\Delta K_{th} = \Delta K_{op} + \Delta K_{th,eff} = \left[1 - e^{-k\cdot(a-a_0)}\right]\cdot \Delta K_{op,max} + \Delta K_{th,eff} \tag{16}$$

but modified by replacing the crack depth a by an equivalent crack depth $\sqrt{area}$ as introduced above. In Eqn. (16) k is a fit parameter which describes how the crack closure effect develops as a function of $a\text{-}a_0$ or $\sqrt{area} - \sqrt{area_0}$ respectively. Since Eqn. (16) includes two fit parameters, k and a_0 or $\sqrt{area_0}$, a minimum of two conditional equations is necessary. The first one is $\Delta K_{th} = 0$ für $\sqrt{area} = 0$; the second on is given by

$$\Delta K_{th} \propto \left(\sqrt{area}\right)^{1/3} \quad , \tag{17}$$

for an arbitrary crack size. For steels, according to [2], Eqn. (17) can be realised by an estimate

$$\Delta K_{th} = 3{,}3\cdot 10^{-3}\left(HV + 120\right)\Big/\left(\sqrt{area}\right)^{1/3} \tag{18}$$

with HV being the Vickers hardness. However, for the aluminium alloy investigated in this study no similar solution exists. Therefore, an alternative solution had to be found which will be described in Section 3.

Fig. (7) graphically shows Eqn. (16) modified for $a \rightarrow \sqrt{area}$. As assumed in [25] the threshold ΔK_{th} is subdivided into an intrinsic value, $\Delta K_{th,eff}$, and an additional amount due to the crack closure effect, $\Delta K_{th,op}$. The intrinsic term is a lower bound which exists even if no crack closure effect occurs (therefore the designation “eff”). It can, e.g., be determined by experiments at different R ratios and extrapolation for $R \rightarrow 1$ as realised in the present paper (Fig. 5).

Because the state of the initial defect is characterised by both, the intrinsic threshold $\Delta K_{th,eff}$ and the initial crack area (respective its square root $\left(\sqrt{area}\right)_i$ the curve according to Eqn. (16) has to be shifted to pass through this point such as shown in the figure. The prediction of the ΔK_{th} versus crack size curve in the component is then provided by the un-dotted dark line. The transition between short and long crack propagation occurs at $\sqrt{area}^*$, where the ΔK_{th} according to the (shifted) Eqn. (9) curve intersects the long crack threshold value.

3. Validation

The validation of the model was performed with specimens identical to those shown in Fig. 3 but prepared with artificial initial defects. Using the FIB (Focus Ion Beam) technology notches with a notch width of 6 μm, a depth of a = 37.4 μm and a length at surface 2c = 101.25 μm were generated (Fig. 8).[1)] The notch dimensions were identical for all validation specimens. With an area of 3230 μm^2 or $\left(\sqrt{area}\right)_i \approx 57\ \mu m$ the size of these artificial defects referred to the upper tail of the statistical distribution of the natural defects found on the fracture surfaces as shown in Fig. 4(d).

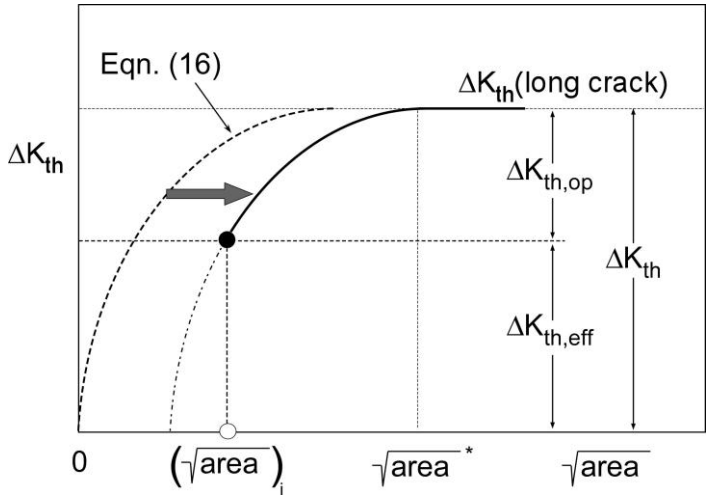

Fig. 7: Proposed method for determining the ΔK_{th}-crack size correlation for short cracks in the present model.

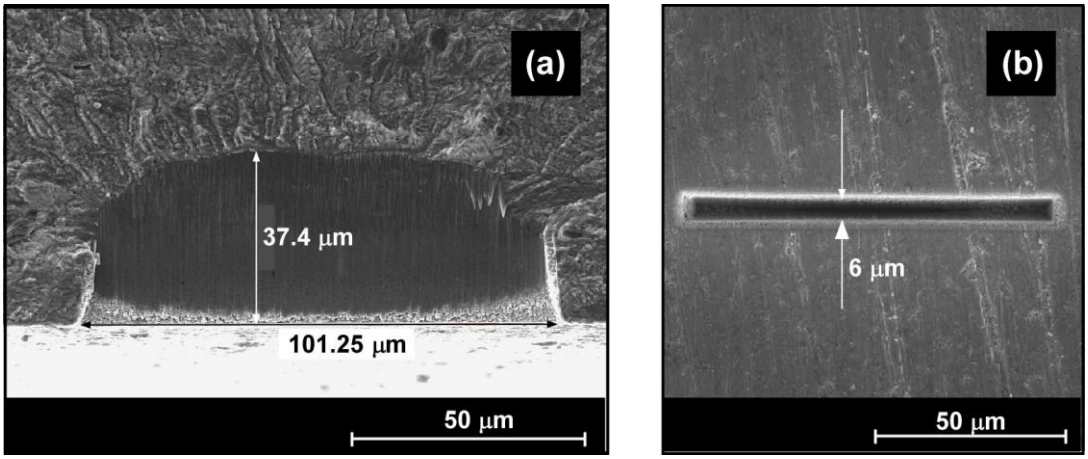

Figure 8: Artificial defect introduced by means of focus ion beam (FIB) technique.

[1)] The authors wish to thank Dr. Erica Lilleodden, HZG Geesthacht, who prepared the FIB cracks.

The prepared specimens were then used to generate an S-N curve. The tests were interrupted when cracks of about 2c = 3 mm were visible at the specimen surfaces. The exact data are summarised in Table 1, the resulting S-N curve is shown in Figure 9.

Table 1: Date of the S-N curve obtained for the tensile plates with artificial (FIB) cracks.

Specimen No.	$\Delta\sigma$ in MPa	N	a at test end in mm	2c at test end in mm
27	179.66	$2.473 \cdot 10^5$	1.23	2.625
28	182.06	$2.019 \cdot 10^5$	1.27	3.15
31	192.4	$1.908 \cdot 10^5$	1.42	3.77
65	202.95	$1.519 \cdot 10^5$	1.15	2.58
66	200.8	$1.444 \cdot 10^5$	0.96	2.35
70*)	163.3	$1.1053 \cdot 10^7$	1.07	2.68
72	163.58	$5.225 \cdot 10^5$	1.27	2.85
75	178.74	$2.244 \cdot 10^5$	1.12	2.85

70) Test interrupted without a visible crack.

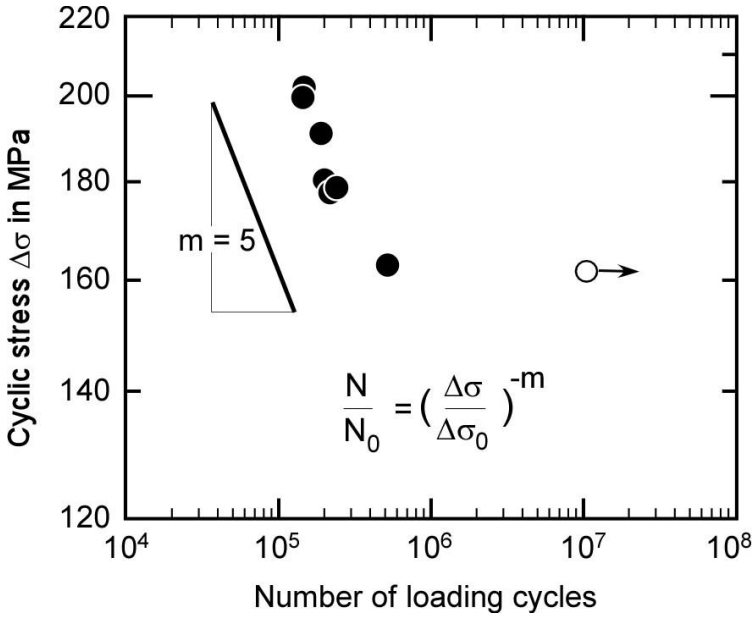

Figure 9: S-N curve obtained for the tensile plates with artificial (FIB) cracks.

The stress-strain data of the material were: cyclic proof strength $R_{p0.2,cyc}$ = 341 MPa and cyclic modulus of elasticity E_{cyc} = 68.4 GPa. For the finite element analysis the stress strain curve was fitted by a Ramberg-Osgood type equation

$$E_{cyc} \cdot \varepsilon = \sigma + \alpha' \cdot \left(\frac{\sigma}{\sigma_{el}} \right)^{n'-1} \cdot \sigma \qquad (19)$$

with $\varepsilon_0 = \sigma_0 / E_{cyc}$, α' = 0.002416, n' = 10.143787 and σ_{el} = 195 MPa.

Further material data such as the da/dN-ΔK curve and the threshold values have been presented in Section 2.2. It has already been mentioned in Section 2.5 that Eqn. (18) was not applicable to the aluminium alloy investigated. Therefore, an alternative second conditional equation had to be used. This is given by a general form of Eqn. (18)

$$\Delta K_{th} = 3.3 \cdot 10^{-3} C_0 \left(\sqrt{area}\right)^{1/3} \tag{20}$$

with $\left(\sqrt{area}\right)_i$ referring to the size of the artificial initial defect and C_0 being a material constant which, according to Murakami [2], correlates with the fatigue limit σ_e (in the present case the fatigue strength at 10^7 loading cycles) by

$$C_0 = \frac{1}{1.43} \sigma_e \left(\sqrt{area}\right)^{1/6}. \tag{21}$$

With σ_e = 80 MPa (Figure 9) and $\left(\sqrt{area}\right)_i$ = 56.85 the parameters in Eqn. (16) have finally been determined as $\left(\sqrt{area}\right)_0$ = 20.86 μm, k = 0.0652 μm^{-1} and $\sqrt{area}^*$ = 140 μm. As mentioned above Eqn. (16) curve had to be shifted such that it passed through the point ($\left(\sqrt{area}\right)_i$, $\Delta K_{th,eff}$). This is realised in Fig. 10.

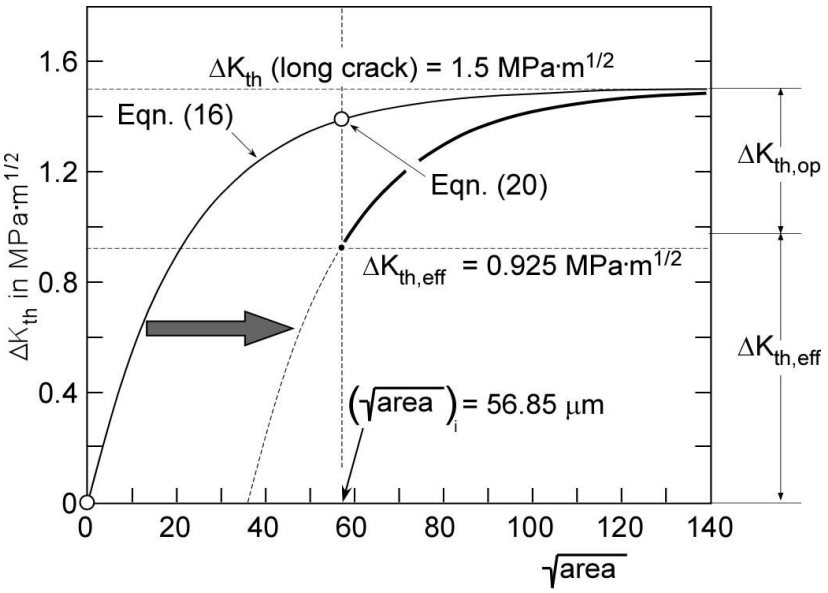

Fig. 10: Application of the model of Figure 7 to the present example.

As the final result the fatigue strength for finite life was predicted as shown in Fig. (11). The analyses were performed for each individual specimen; therefore, the presentation of the results as continuous straight line is not quite correct. However, the points were so close to a straight line that this was used for simplification. In addition the predicted and experimental values of the crack size, a and 2c, at test end, are compared in Fig. 11. It shows up that all experimental data were predicted with satisfying accuracy.

4. Summary and Outlook

An analytical fracture mechanics model for predicting the finite life fatigue strength range of the S-N curve was developed. Its application was demonstrated for small plates made of aluminium Al 5380 H321 and loaded in tension. The results were promising.

The model is based on a number of assumptions:

(a) In engineering materials fatigue crack propagation initiates at pre-existing material defects such as welding flaws, pores, inclusions etc.

(b) The crack initiation sub-stage in a narrower sense during which a crack develops from the pre-existent defect is typically rather limited. Therefore, a fracture mechanics based lifetime prediction (which per definition is a residual lifetime prediction) yields conservative but not over-pessimistic lifetimes. Note, however, that this has not to be the case for any material.

(c) The initial crack size has to be obtained individually and not by back-calculation. For this purpose the fracture surfaces of cyclically loaded specimens were investigated in the present study. Note, however, that such a high effort is not realistic for most practical cases because of which rules for fixed initial crack sizes have to be worked out for future application in the frame of a potential assessment procedure.

(d) Since the major part of lifetime belongs to short crack propagation specific issues such as the transient behaviour of crack closure of short cracks and local ligament plasticity effects had to be taken into account.

(e) The presented model is limited to the propagation of mechanically short cracks and not applicable to micro-structurally short ones.

(f) Fracture mechanics based determination of fatigue strength provided significant potential as compared to and in addition to classical fatigue strength concepts because it takes parameters such as weld geometry, residual stresses etc. explicitly into account.

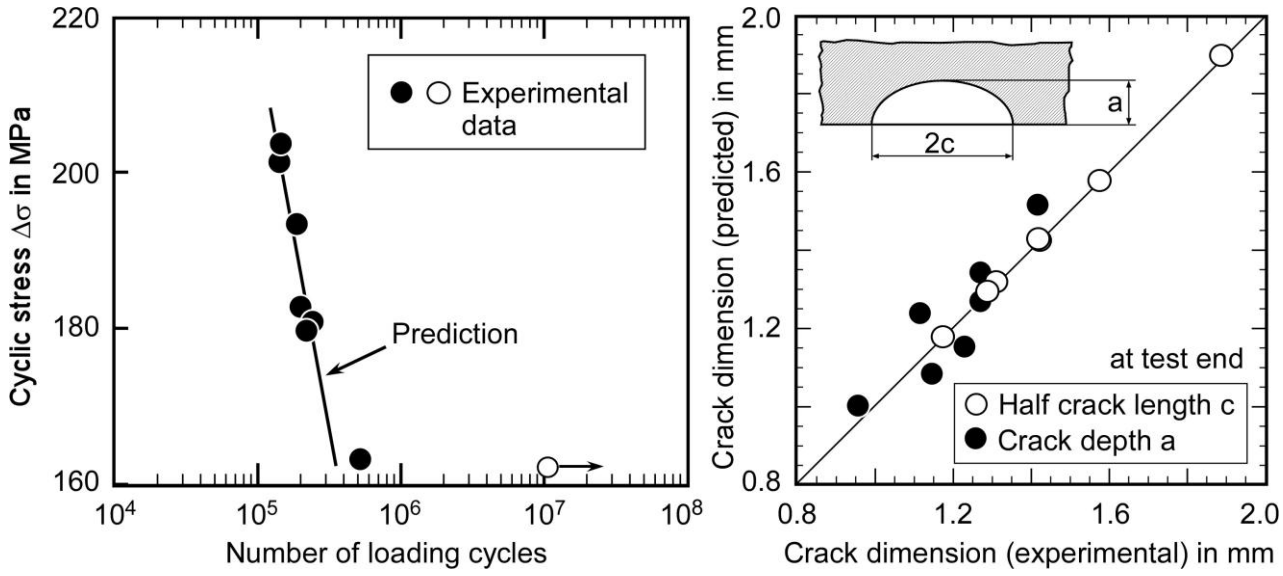

Fig. 11: S-N curve obtained for the tensile plates with artificial (FIB) cracks. Comparison between the experiments and the predictions with the present model.

Literature

[1] Polak, J. (2003): Cyclic deformation, crack initiation, and low-cycle fatigue. In: Ritchie, R.O. and Murakami, Y. (Eds.): Comprehensive Structural Integrity; Volume 4: Cyclic loading and Fracture; Elsevier, 1-39.

[2] Murakami, Y. (2003): High and ultrahigh cycle fatigue. In: Ritchie, R.O. and Murakami, Y. (Eds.): Comprehensive Structural Integrity; Volume 4: Cyclic loading and Fracture; Elsevier, 41-76.

[3] Miller, K.J. and O'Donnel, W.J. (1999): The fatigue limit and its elimination. Fatigue & Fracture of Engng. Mater. & Struct. 22, 545-557.

[4] Tanaka, K. (2003): Fatigue crack propagation. In: Ritchie, R.O. and Murakami, Y. (Eds.): Comprehensive Structural Integrity; Volume 4: Cyclic loading and Fracture; Elsevier, 95-127.

[5] Zerbst, U., Madia, M. und Hellmann, D. (2011): An analytical fracture mechanics model for estimation of S-N curves of metallic alloys containing large second particles. Engng. Fracture Mech. 82, 115-134.

[6] Ishihara, S. and McEvily, A.J. (2002): Analysis of short crack growth in cast aluminium alloys. Int. J. Fatigue 24, 1169-1174.

[7] Bruzzi, M.S. and McHugh, P.E. (2002): Methodology for modelling the small crack fatigue gehaviour of aluminium alloy. Int. J. Fatigue 24, 1071-1078.

[8] McClung, R.C., Chell, G.G., Lee, Y.-D., Russel, D.A. und Orient, G.E. (1997): A practical methodology for elastic-plastic fatigue crack growth. ASTM STP 1296, 317-337.

[9] Eufinger, J., Heinrietz, A., Bruder, T. und Hanselka, H. (2010): Bruchmechanisch basierte Schwingfestigkeitsanalyse von Gusseisen unter Berücksichtigung der Gefügeeigenschaften. 43. Tagung des DVM-Arbeitskreises "Bruchvorgänge, DVM-Bericht 243, 203-213.

[10] Rudd, J.L. and Gray, T.D. (1976): Equivalent initial quality method. Technical Report AFFDL-TM-76-83, US Airforce Flight Dynamics Laboratory.

[11] White, P. (2006): Review of methods and approaches for the structural risk assessment of aircraft. Australian Defence Science and Technology Organisation, Victoria, Australia, http://www.dtic.mil/cgi-bin/GetTRDoc?Location=U2&doc= GetTRDoc.pdf&AD=ADA462955

[12] Raju, I.S. and Newman, J.C., Hr. (1979): Stress-intensity factors for a wide range of semi-elliptical surface cracks in finite-thickness plates. Engng,. Fracture Mech. 11, 817-829.

[13] Zerbst, U., Ainsworth, R.A. und Madia, M. (2011): Reference load versus limit load in engineering flaw assessment: A proposal for a hybrid analysis option. Engng. Fracture Mech., upcoming.

[14] R6, Revision 4 (2009): Assessment of the Integrity of Structures Containing Defects. British Energy Generation Ltd (BEGL), Barnwood, Gloucester.

[15] Zerbst, U., Schödel, M., Webster, S. and Ainsworth, R.A. (2007): Fitness-for-Service Fracture Assessment of Structures Containing Cracks. A Workbook based on the European SINTAP/FITNET Procedure. Elsevier.

[16] Newman, J.C., Jr. (1984): A crack opening stress Equation for fatigue crack growth. Int. J. Fracture 24, R131-R135.

[17] Beretta S., Carboni, M. and Madia, M. (2006): Fatigue Strength in Presence of Inhomogeneities: Influence of Constraint. Journal of ASTM International. Vol. 3, No. 4.

[18] McClung, R.C., Chell, G.G., Lee, Y.-D., Russel, D.A. und Orient, G.E. (1997): A practical methodology for elastic-plastic fatigue crack growth. ASTM STP 1296, 317-337.

[19] McClung, R.C., Chell, G.G., Lee, Y.-D., Russell, D.A. and Orient, G.E. (1999): Development of a practical methodology for elastic-plastic and fully plastic fatigue crack growth. NASA Report NASA/CR-1999-209428.

[20] Fatigue crack growth computer program "NASGRO" Version 3, NASA, Houston, Texas, 2000.

[21] Newman, J.C., Jr. (1984): A crack opening stress Equation for fatigue crack growth. Int. J. Fracture 24, R131-R135.

[22] McClung, R.C (1994): Finite element analysis of specimen geometry effects on fatigue crack closure. Fatigue Fracture Engng. Mat. Struct. 17, 861-872.

[23] Liu, J.Z. and Wu, X.R. (1997): Study of fatigue crack closure behaviour for various cracked geometries. Engng. Fracture Mech. 57, 475-491.

[24] Kim, J.H. and Lee, S.B. (2000): Fatigue crack opening stress based on the strip-yield model. Theor. Appl. Fracture Mech. 34, 73-84.

[25] McEvily, A.J., Endo, M. and Murakami, Y. (2003): On the $\sqrt{area}$ relationship and the short fatigue crack threshold. Fatigue Fracture Engng. Mat. Struct. 26, 269-278.

[26] Murakami, Y. (2002): Effects of nonmetallic inclusions on fatigue strength. In: Murakami, Y.: Metal Fatigue: Effects of small defects and non-metallic inclusions. Elsevier, Amsterdam et al., Chapter 6, 75-127.